



THE UNIVERSITY *of* EDINBURGH

Edinburgh Research Explorer

## Effect of spacer length on the performance of peptide-based electrochemical biosensors for protease detection

### Citation for published version:

González-fernández, E, Staderini, M, Avlonitis, N, Murray, AF, Mount, AR & Bradley, M 2017, 'Effect of spacer length on the performance of peptide-based electrochemical biosensors for protease detection', *Sensors and Actuators B: Chemical*. <https://doi.org/10.1016/j.snb.2017.09.128>

### Digital Object Identifier (DOI):

[10.1016/j.snb.2017.09.128](https://doi.org/10.1016/j.snb.2017.09.128)

### Link:

[Link to publication record in Edinburgh Research Explorer](#)

### Document Version:

Peer reviewed version

### Published In:

Sensors and Actuators B: Chemical

### General rights

Copyright for the publications made accessible via the Edinburgh Research Explorer is retained by the author(s) and / or other copyright owners and it is a condition of accessing these publications that users recognise and abide by the legal requirements associated with these rights.

### Take down policy

The University of Edinburgh has made every reasonable effort to ensure that Edinburgh Research Explorer content complies with UK legislation. If you believe that the public display of this file breaches copyright please contact [openaccess@ed.ac.uk](mailto:openaccess@ed.ac.uk) providing details, and we will remove access to the work immediately and investigate your claim.



## Effect of Spacer Length on the Performance of Peptide-Based Electrochemical Biosensors for Protease Detection

Eva González-Fernández,<sup>a§</sup> Matteo Staderini,<sup>a§</sup> Nicolaos Avlonitis,<sup>a</sup> Alan F. Murray,<sup>b</sup> Andrew R. Mount,<sup>a\*</sup>, Mark Bradley<sup>a\*</sup>

<sup>a</sup> EaStCHEM, School of Chemistry, University of Edinburgh, Joseph Black Building, West Mains Road, Edinburgh, EH9 3FJ, UK.

<sup>b</sup> School of Engineering, Institute for Bioengineering, The University of Edinburgh, The King's Buildings, Mayfield Road, Edinburgh EH9 3JL, UK.

<sup>§</sup>These authors contributed equally to this study

\*Corresponding authors. Fax: 0044 131 777 0334

E-mails: [mark.bradley@ed.ac.uk](mailto:mark.bradley@ed.ac.uk); [a.mount@ed.ac.uk](mailto:a.mount@ed.ac.uk)

### Abstract

Peptide-based electrochemical biosensors typically consist of a short peptide sequence, labelled with a redox reporter and modified with a thiol-containing moiety to allow immobilisation onto a gold electrode surface. A spacer is often introduced between the thiol group and the peptide with the aim of promoting enzyme accessibility as well as conferring flexibility onto the probe. Herein we report a systematic study of the effect of polyethylene glycol (PEG)-based spacer length on the performance of such biosensors in order to gain a deeper understanding of their role and optimise a peptide-based electrochemical sensor. Thus a specific peptide endowed with varying PEG spacers (PEG-4, PEG-6, PEG-8 and PEG-12) were synthesised and interrogated by the addition of both a target enzyme (trypsin) and BSA in order to evaluate their analytical performance. An alkyl-based spacer was also assessed in order to compare the effect of the nature of the spacer. All of the proposed probes supported efficient protease detection; however, PEG-6 provided enhanced anti-fouling properties, which highlights the vital role of the spacer in the design of peptide-based probes.

## *Keywords*

Peptide-based probe

Electrochemical detection

Protease detection

Polyethylene glycol spacer (PEG)

## **1. Introduction**

Proteases play a pivotal role in many physiological processes and their deregulation has been associated or implicated in a huge number of maladies. For example, it has been well established that the proteolytic activity of both intracellular and extracellular proteases, such as matrix metallo-proteinases (MMPs), contributes to cancer progression in all its stages (e.g. tumour angiogenesis, invasion and metastasis) [1, 2]. Furthermore, there is much evidence which shows that caspases are critical for the activation of the apoptotic pathway [3]. In the light of these findings, a broad variety of proteases have been recognised as potential diagnostic targets, increasing the demand for selective and sensitive tools for their detection in a biomedical setting.

In this context, electrochemical biosensors, with their high sensitivity, low limits of detection and ease of miniaturisation, are valuable tools for the direct assessment of cancer biomarkers [4-6]. Interestingly, a common strategy to produce selectivity in electrochemical biosensors is the use of peptides as recognition moieties, designed to interact with specific analytes including antibodies and enzymes [7, 8]. Building on this approach, electrochemical peptide-based biosensors have been successfully generated for the detection of protease activity [9-14]. Most of these consist of a simple peptide, which acts as substrate for the target enzyme, which is labelled with a redox reporter and immobilised onto an electrode surface. Upon enzymatic cleavage the redox-labelled probe fragment is released from the electrode surface leading to a measurable signal decrease. It has been shown that the insertion of a flexible spacer within this probe can facilitate the approach of the redox

reporter to the electrode, thereby facilitating electron transfer and enhancing the redox signal [9, 10]. With this in mind, we recently developed an electrochemical peptide-based biosensor with a polyethylene glycol (PEG) spacer and methylene blue as redox reporter [11].

However, the conformation and orientation of peptides immobilised onto a solid surface are both critical for analyte detection and these can be significantly influenced by the spacer [15]. There is also a growing body of data showing that different spacer lengths vary the signal response of the biosensor by altering the properties of the recognition moiety [16-18]. For example, Martić reported an electrochemical study of a series ferrocene-ATP bioconjugates, which showed that structural variation of the length of an alkyl linker modulated the detection and quantification of kinase activity [19], with a longer alkyl spacer facilitating the interaction with the binding site of the enzyme through reducing the steric hindrance. Despite this fact, no systematic exploration of the effect of different spacer lengths on their analytical performance has been carried out.

In the light of these findings, and in an effort to further enhance the analytical properties of our system, here we explore the effect of different lengths of the PEG-spacer connecting the anchor moiety to the peptide sequence. This systematic study describes the effects of varying the length of PEG-spacers (PEG-4, PEG-6, PEG-8, PEG-12) on the probe performance, with special emphasis on their ability to tune the anti-fouling capabilities of the resulting sensing films. Indeed, improvements in a sensing platform to prevent non-specific binding to the probe film surface are of a paramount importance for the development of self-assembled monolayer (SAM)-based electrochemical biosensors. To address this aim, different strategies have been proposed including ternary SAMs, T-SAMs, which consist of the immobilisation of three components: the probe plus two backfilling molecules (co-adsorbents), that have successfully increased prevention of non-specific binding [11, 20-25]. The present study offers a deeper understanding of how the length of the PEG-based spacer affects the specificity and sensitivity of the probe, providing fundamental insights for the design of advanced new protease biosensors.

## **2. Materials and Methods.**

### *2.1. Instrumentation*

Electrochemical measurements were performed using a conventional three-electrode electrochemical cell driven by a computer-controlled AutoLab PGstat-30 potentiostat running the GPES 4.9 software (EcoChemie, The Netherlands). A platinum wire and a 2 mm diameter polycrystalline gold electrode (IJ Cambria, UK) were used as auxiliary and working electrode, respectively. All the potentials were measured using, and are referred to, the Ag | AgCl | KCl (3 M) reference electrode (Bioanalytical Systems, Inc., USA).

### *2.2. Reagents*

Trypsin (MW 23.4 KDa), bovine serum albumin (BSA), 6-mercaptohexanol (MCH), 2,2'-(ethylenedioxy)diethanethiol (PDT) and 10x PBS were purchased from Sigma Aldrich (UK) and used as received. All reagents were of analytical grade. All solutions were prepared using protease-free deionised water.

### *2.3. Experimental methods*

#### *2.3.1. Synthesis*

The detailed synthetic experimental procedures are described in Appendix A: Supplementary Material.

#### *2.3.2. Electrode cleaning and pre-treatment*

After immersing in the minimum volume of piranha solution (3:1-H<sub>2</sub>SO<sub>4</sub> (95%): H<sub>2</sub>O<sub>2</sub> (33%)) (CAUTION: piranha solution is strongly oxidising and should be handled with care!) for 10 min in order to eliminate any organic matter from the gold surface, the working electrode was successively polished on a polishing cloth using alumina slurries of 1, 0.3 and 0.05 µm particle size (Buehler, Germany). This working electrode was then further cleaned by immersion in H<sub>2</sub>SO<sub>4</sub> (95%) and then HNO<sub>3</sub> (65%) at room temperature for 10 min. Finally, the working electrode was subjected to cyclic voltammetry, carrying out potential cycles

between 0 and +1.6 V in 0.1 M H<sub>2</sub>SO<sub>4</sub> at a scan rate of 100 mV·s<sup>-1</sup> until the characteristic voltammogram of clean polycrystalline gold was obtained [26].

For surface roughness calculation, the real or effective electrode area was calculated from the charge related to the gold oxide reduction peak from the former voltammogram, and using 400 μC/cm<sup>2</sup> (charge corresponding to desorption of a monolayer of gold oxide on polycrystalline gold) to convert the charge value into real area.

#### *2.3.3. Sensing phase - preparation protocol*

The sensing phase was formed as a mixed SAM on the gold electrode surface by immersing the freshly cleaned and pre-treated gold working electrode overnight at 4 °C in a 40 μM solution of the redox-labelled peptide (substrate, L-amino acids or control, D-amino acids) and freshly prepared PDT (600 μM) in ethanol. After washing with ethanol, the resulting SAM-modified electrode was immersed in 1 mM MCH in ethanol for 1 hour at room temperature. Finally, two washing steps were carried out, first in ethanol and then in phosphate-buffered saline (PBS). The modified electrodes were then stored in PBS solution at 4 °C until use.

#### *2.3.4. Sensor measurements*

The modified electrodes were immersed in 1x PBS buffer solution and electrochemically interrogated using square wave voltammetry (SWV, at a frequency of 60 Hz, amplitude of 25 mV and step potential of 5 mV) until a stable background signal was obtained. After addition of the target enzyme, the SWV signal was continuously monitored with time, with the resulting signal gain being expressed as the relative change in the SWV peak current with respect to the initial peak current (henceforth called the % signal change).

### **3. Results and discussion**

To study the influence of the length of the spacer on the peptide-based electrochemical biosensor, a series of specific peptide-based probes were synthesised with methylene blue as redox tag and a terminal cysteine to anchor the probe to the electrode surface (via an S-Au bond). Each contained a PEG spacer of a specific number of ethylene glycol units (2, 4, 6, 8 and 12) (Figure 1A) and a cleavable short peptide sequence (for trypsin) (Phe-Arg-Arg (FRR)). Their respective performances as an electrochemical protease detection platform were evaluated in parallel and compared to previously reported results. In all cases the equivalent uncleavable D-amino acid-based probe was also synthesised, which constituted a negative control.

The sensing phase was formed through immobilisation of the appropriate peptide-based probe on the gold electrode, in a ternary-SAM (T-SAM) configuration [11, 20, 21], using PEG-based dithiol and mercaptohexanol as co-adsorbents. Previous work from our group [11] showed the suitability and stability of the T-SAM platform with respect to quantitative electrochemical peptide-based protease biosensing. These SAM-modified surfaces were electrochemically interrogated before and during their incubation with the target protease, which leads to enzyme-catalysed cleavage and release of the redox-containing fragment into solution (Figure 1B). This causes a decrease of peak current measured by SWV, which here is reported as % signal change (the relative decrease in SWV peak current with respect to the initial SWV peak current recorded, expressed as a percentage, prior to enzyme addition.)

The choice of PEG-based moieties as spacers for the proposed sensing platform were based on previous work from our group, where we compared, side by side, the performance of two similar peptide-based probes for the analysis of trypsin, one containing a PEG-based spacer and the other an alkyl-based spacer, both with ferrocene as redox tag [11]. This showed that a PEG-based spacer enhanced the performance of the sensor, with two possible explanations, namely increased hydrophilicity of the PEG-chains that promoted mobility and biomolecular interactions or the formation of a less packed SAM, giving greater spacing between immobilised probes. In order to confirm that the PEG-based spacers

showed enhanced performance the present study included an alkyl-based spacer analogue to the PEG-2 probe (Figure 1A), where the PEG spacer was replaced with an alkyl chain (8-aminooctanoid acid, Aoc).

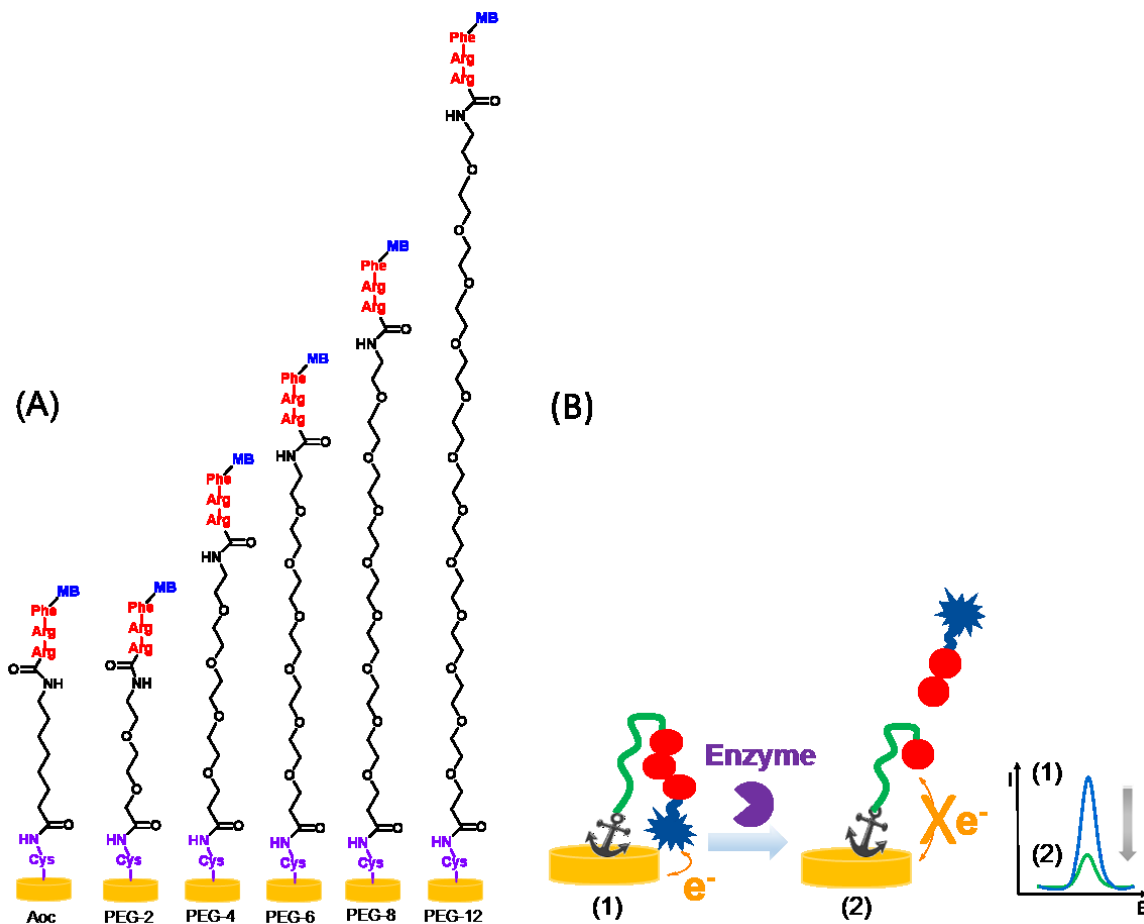


Figure 1. (A) Chemical structures of the different probes, each containing one of five PEG spacer lengths, with the number of EG units, denoted by PEG-*x*, or an alkyl-based spacer containing 8-aminooctanoid acid, Aoc. (B) Principle of detection for the peptide-based electrochemical platform. The protease enzyme (trypsin) catalyses the cleavage of the immobilised redox-labelled peptide (1), releasing the redox-containing fragment into solution (2), leading to a decrease of the electrochemical signal, observed by decrease in the SWV peak current.



### 3.1. Effect of varying PEG-based spacer length on the initial current and the maximum % signal change recorded

The proposed platform generates a real-time *signal-off* response, meaning that the presence of the protease causes a decrease in the measured SWV peak current, as this is related to the electrochemical reduction of the remaining methylene blue moieties attached to the electrode surface through the peptide-based probe. Interestingly, this decreasing signal never reaches zero (when expressed as % signal change it never gets to 100%), suggesting that a subset of the redox-tagged peptides are not accessible for enzyme cleavage. We therefore tested the effect of increasing the PEG-based spacer length on both the initial current and the maximum % signal change recorded upon the addition of a high concentration of trypsin to explore any variation in probe orientation and accessibility.

Both substrate and control-modified T-SAMs were prepared for all probes synthesised and their initial signal evaluated in PBS by means of SWV. Figure 2 shows representative voltammograms recorded in PBS prior to the addition of enzyme (Figure 2A) and the average initial currents (Figure 2B) for all the various PEG-based spacers under evaluation. Initial peak currents were seen to be significantly decreased for the two longest PEG-spacer lengths compared to the three shortest spacer lengths, with at least a 2-fold decrease when changing from the group (PEG-2, PEG-4 and, PEG-6) to (PEG-8 and PEG-12), the initial current values recorded for each different group are considered to be equal within the experimental error. This is consistent with the hypothesis that the longest spacer lengths lead to less efficient redox transfer between the methylene blue and the electrode surface. Furthermore, a T-SAM prepared with the alkyl-based probe was also evaluated. The initial current registered was comparable to the one corresponding to the PEG-2 analogue spacer (Figure 2B), confirming the ability of both spacers to allow efficient redox transfer between the redox reporter and the electrode surface.

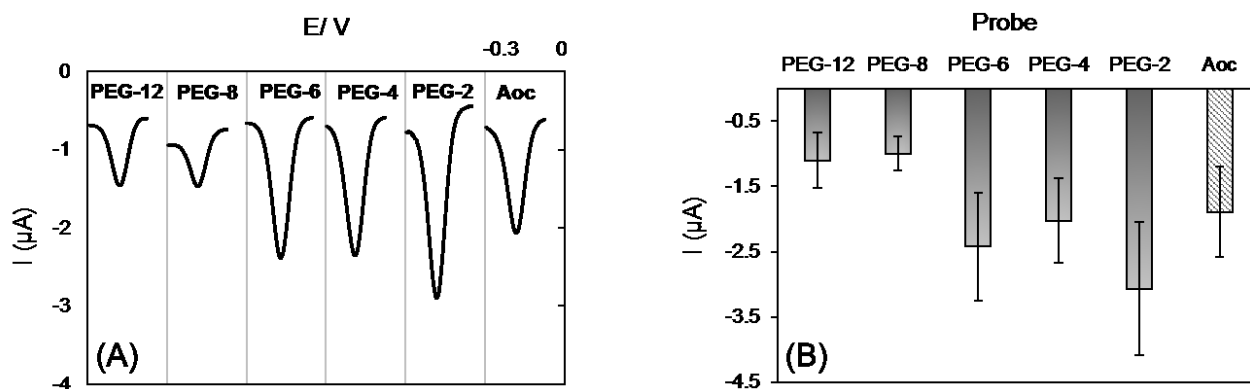


Figure 2. (A) Typical SWV data registered for a T-SAM prepared using the denoted PEG-based or Aoc spacer probes without target enzyme in PBS. (B) Average initial SWV peak current registered for each different probes under evaluation (average values and error bars calculated from at least 10 individual sensing SAM layers).

The substrate and control-modified T-SAMs were then incubated with trypsin and the signal changes monitored over time by SWV. As shown in Figure 3, the maximum % signal change registered for the substrate-modified T-SAMs (Figure 3, grey columns) was the same within experimental error for all the PEGs used, indicating that probe accessibility does not depend significantly on PEG spacer length, and that approximately half of the surface-bound probes are cleavable. A possible explanation for this effect could be due to the surface roughness of the gold electrodes used (defined as the ratio between the real and the geometrical area). The fraction of probes located in the “corrugations” of the electrode surface that lead to such roughness may well not be accessible to the enzyme, and thus will not be cleaved, resulting in a residual current. This explanation was previously envisioned and confirmed by a ferrocene-tagged peptide-based protease sensor for thrombin [10]. In this case, the use of ultra flat gold electrodes led to % signal change larger than 90%, that clearly differ from the typically 60% signal change recorded for the polished gold surfaces. In this context, the

electrochemically assessed roughness factor for the polished gold electrodes used throughout this study was found to be  $3.2 \pm 0.8$  (see section 2.3.2 for calculation protocol), which is in agreement to the values reported for the study mentioned above [9], confirming lack of accessibility as a plausible explanation for this effect. In contrast, the variation in the response observed for the control-modified T-SAMs (Figure 3, hatched columns) was significant, with PEG-6 producing the smallest % signal change within the negative controls, while PEG-8 produced the largest. This is an interesting finding that we attribute to differences in the internal SAM structure for the different PEG spacers.

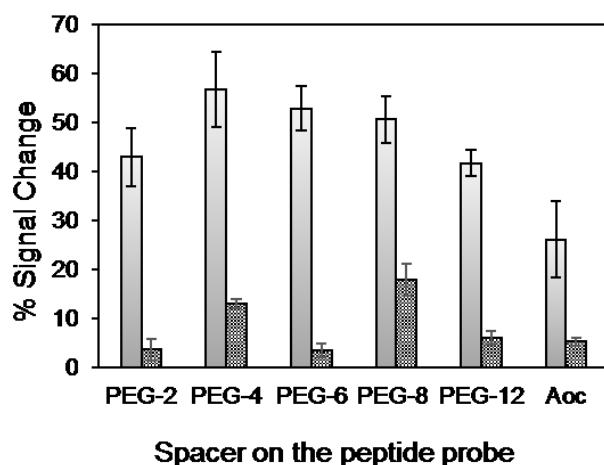


Figure 3. % Signal change registered for different T-SAMs prepared with the various peptide probes containing the different PEG-based spacer lengths or Aoc probe and incubated with trypsin (100 nM) for substrate-modified T-SAMs (grey columns) and control-modified T-SAMs (hatched columns). Data and error bars are typically from 3 individual SAM sensing layers.

Additionally, a direct comparison with the alkyl-based spacer showed that this probe allowed the lowest % signal change registered upon addition of trypsin when compared with the

PEG-based probes, confirming that PEG-based probes are able to form a sensing film that promotes enzyme cleavage, as reported previously for ferrocene-tagged peptides [11].

### *3.2. Analytical performance comparison for T-SAMs prepared with varying PEG-based spacer length probes as electrochemical platforms for trypsin detection*

All four surfaces (comprising the different probes (PEG-4 to PEG-12)) were assessed and compared to the previously reported PEG-2 spacer. For this purpose the sensing platforms were immersed in solutions containing varying trypsin concentrations (0.1-100 nM) and the electrochemical signal monitored in real-time, expressed as % signal change. Plotting the % signal at the end point of the incubation (at 90 min, taken as a practical maximum timescale of detection) against the logarithm of the concentration of trypsin showed a linear relationship, allowing each of the sensing platforms to be evaluated and compared. Their analytical characteristics are compiled in Table 1. Limits of detection (LoD), calculated as the enzyme concentration corresponding to 90% of the initial signal value, and dynamic range proved the ability of all probes to support protease detection in a clinically-relevant range (5-15 nM for healthy individuals and 34-85 nM in the case of pancreatic conditions) [27]. The lowest LoD (for PEG-4) was around one order of magnitude lower than that for the highest (the PEG-8 probe) and was four times lower than that for PEG-2. This is an interesting finding, as the % signal change values for a high trypsin concentration registered for these two probes (PEG-4 and PEG-8) were similar (Figure 3). PEG-4 demonstrated the highest % signal change recorded when using a high (100 nM) trypsin concentration, which translated into higher % signal change differences for the same trypsin concentration compared to the other probes, and thus a lower LoD. However, the optimum sensing platform was selected taking into consideration additional parameters such as the minimisation of non-specific adsorption, as discussed in section 3.3. Quantitative kinetic analysis of the signal decrease was also carried out for each of the probes. The data were fitted to a Michaelis-Menten cleavage model previously used [11] and allowed the extraction of an effective reaction rate

constant,  $k_{eff}$ , for each of the concentrations tested. Comparison of the calculated  $k_{eff}$  for the catalytic activity of trypsin 100 nM towards each probe showed comparable cleavage rates for PEG-2, PEG-4 and PEG-6 and a slightly but significantly lower rate for PEG-8 and PEG-12 (Table 1).

Table 1. Analytical performance and kinetic analysis comparison for trypsin protease sensors endowed with varying PEG-based spacer lengths.

Probe (spacer)	LoD (pM)	Dynamic range (nM)	CV% for [trypsin]=100 nM	$k_{eff}$ (min <sup>-1</sup> ) for [trypsin]=100 nM
<b>T-PEG-2</b> <sup>(1)</sup>	250	0.1-100	4	0.080±0.007
<b>T-PEG-4</b>	88	0.1-100	7	0.068±0.005
<b>T-PEG-6</b>	197	0.1-100	7	0.060±0.004
<b>T-PEG-8</b>	789	1-25	6	0.043±0.001
<b>T-PEG-12</b>	252	1-100	7	0.045±0.004

<sup>(1)</sup> Data from reference [11]. CV%: coefficient of variation.

### 3.3. Effect of increasing PEG-based spacer length on anti-fouling properties

Non-specific binding can compromise the successful exploitation of reagent-less electrochemical platforms, which rely on a *signal-off* output [28]. This arises from the intrinsic nature of the signal source; a decrease when the target analyte (in this case enzyme) concentration increases renders it difficult to distinguish between a specific (in this case enzyme cleavage) event and a non-specific binding event onto the sensing platform, (such as the reduction of methylene blue accessibility to the electrode due to restriction of tethered probe flexibility).

We therefore investigated the ability of our probes (PEG-4, PEG-6, PEG-8 and PEG-12) to vary the anti-fouling capability of the employed T-SAM sensing platform for protease detection. The non-specific binding for each of the T-SAMs prepared with such probes was

assessed by monitoring the electrochemical signal change upon addition of bovine serum albumin (BSA). Furthermore, we also evaluated the alkyl-based probe (Aoc) and compared its anti-fouling properties to the PEG-based spacers. Figure 4 depicts the % signal change registered for substrate-modified surfaces for the specific interaction with 100 nM trypsin (grey columns) compared to the % signal change registered upon the addition of 100 nM BSA (dotted columns). As mentioned before, the decrease of the former SWV signal change is due to the specific interaction arising from the release of the methylene blue-containing peptide fragment into solution as a consequence of the catalytic cleavage of the substrate probe by trypsin. For the latter signal change, the registered signal decrease was attributed to the reduced probe flexibility caused by BSA non-specific adsorption on the probe-modified surface, which hindered the redox tag in its approach to the electrode surface. Reassuringly, for all the different PEG-based lengths tested, the % signal change registered was larger for the specific interaction with trypsin than for the non-specific one with BSA. However, it is important to note that the magnitude of the non-specific binding varies with the PEG-based spacer length, with the minimum for the PEG-6 probe corresponding to less than half the value recorded for both PEG-12 and PEG-2 analogues. Figure 4 also depicts the fraction of the specific versus the non-specific signal, as a means of quantifying the degree of anti-fouling ability for each probe. From the data, it emerges that changing the length of the PEG-based spacer allows tuning of the anti-fouling capability of the T-SAMs, with PEG-6 offering the best spacer length, conferring the sensing platform minimum non-specific binding interaction, thereby assuring that the maximum signal registered is due to the specific catalytic cleavage from trypsin. It is also significant that the alkyl-based probe showed the poorest anti-fouling properties, indicated by the lowest specific/non-specific signal ratio, supporting the hypothesis that having a PEG-based spacer contributes to the minimisation of non-specific interactions on the sensing surface.

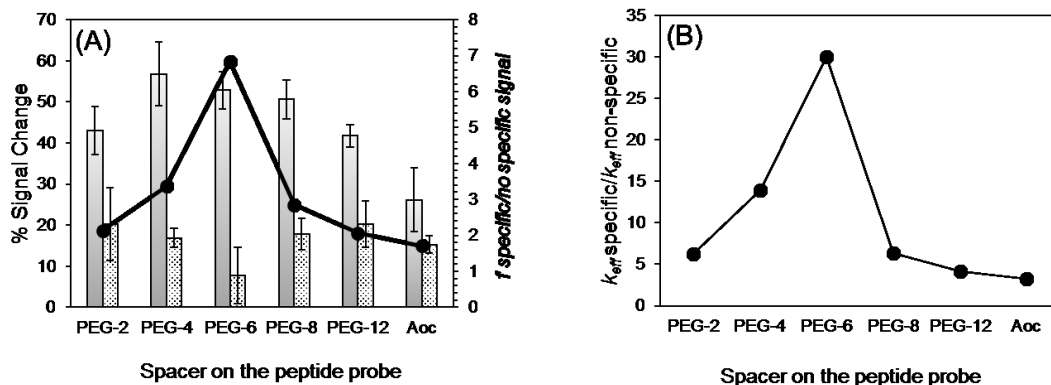


Figure 4. (A) Percentage signal change for the specific interaction registered upon addition of trypsin 100 nM (grey columns) or for the non-specific interaction with BSA 100 nM (dotted columns) after 70 min incubation. Black line = specific versus non-specific ratio registered for each probe. Data and error bars are typically from 3 individual SAM sensing layers. (B) Ratio for the measured effective reaction rate constant,  $k_{\text{eff}}$ , for the specific (trypsin 100 nM) and non-specific (BSA 100 nM) binding.

Additionally, as with the enzyme studies above, the kinetics of the signal change caused by non-specific adsorption were also evaluated. Data corresponding to the incubation of each individual sensing platform, prepared with the different probes, with 100 nM BSA were fitted to the same Michaelis-Menten kinetics model as for the enzyme cleavage studies, allowing the extraction of an effective reaction rate constant,  $k_{\text{eff}}$ , for each case. PEG-2, PEG-4, PEG-6 and alkyl-based (Aoc) probes showed a good fitting to the mentioned model, whereas PEG-8 and PEG-12 appeared to have different time dependences for non-specific binding signal changes. A direct comparison of the measured  $k_{\text{eff}}$  for both trypsin and BSA 100 nM for each probe showed PEG-6 to exhibit not only the smallest but also the slowest non-specific binding of BSA compared to trypsin, data that confirms the optimal anti-fouling ability of this probe. Once more, the alkyl-based probe showed the poorest performance, presenting the fastest non-specific binding of BSA compared to enzymatic trypsin cleavage.

Finally, with the aim of gaining a further understanding on how the different spacers affect the hydrophilic/hydrophobic balance of the SAM-modified electrode surfaces the contact angle for each of the T-SAMs prepared with the different probes under study was analysed. Interestingly, the measured contact angles (see supporting material) showed no significant differences among the various probes tested, suggesting that the peptide moiety dominates the external region of the sensing film. This finding reinforces the hypothesis that when a protein (here trypsin or BSA) reaches the sensing surface there are no significant differences on this outer layer dependant on the spacer. We suggest that the differences in performance in the present study for the various spacers are based on how these spacers promote/hinder the accessibility to the inner part of the SAM, facilitating access to the cleaving site for trypsin while preventing the non-specific binding of other proteins, such BSA to the interior. Thus a molecule of BSA that reaches the outer part of the sensing film has hindered access to the inner part of the film, preventing it from forming non-specific interactions depending on the nature of the spacer (an alkyl-based spacer shows the poorest specific/non-specific signal ratio in comparison to PEG-based spacers) and the length of the PEG moiety, reaching its optimum length at PEG-6. In line with this, PEG-2 and PEG-4 seem not long enough to prevent non-specific adsorptions, while PEG-6 appears to give the surface optimum anti-fouling capabilities. Increasing the PEG length (PEG-8 and PEG-12) did not translate in enhanced performance, maybe due to enhanced flexibility that can also facilitate access to the inner part of the sensing film.

#### **4. Conclusions**

We have presented a systematic study of protease detection using a peptide-based electrochemical biosensor platform, whose signal arises from the loss of the redox tag caused by specific catalytic cleavage of the peptide substrate, concentrating on the effect of the spacer length. Various probes were synthesised, endowed with PEG-based spacers of different lengths and immobilised in a T-SAM configuration onto a gold surface. An alkyl-based spacer analogue probe was also synthesised in order to compare the effect of the



nature of the spacer. The ability of all the proposed probes to support efficient trypsin detection was assessed and compared to previously reported results. It rapidly became clear that increasing the length of the spacer led to a decrease of the initial current registered by means of SWV for PEG-8 and PEG-12 when compared to PEG-2, PEG-4 and PEG-6. Nevertheless, a comparable maximum % signal decrease was registered for all probes upon incubation with a high trypsin concentration, suggesting that PEG length does not have a strong influence on probe accessibility. All probes exhibited suitable analytical performance in terms of LoD, ranging from 90-800 pM. Interestingly PEG-6 showed the highest maximum % signal change for the substrate probes. It also displayed the minimum response for the negative control experiments and upon incubation of a non-specific protein (BSA), showing that differences in PEG-based spacer length can “tune” the anti-fouling properties of the sensing platform. On the contrary, the alkyl-based probe rendered the poorest anti-fouling abilities, confirming the nature of the spacer also plays an important role additionally to its length. In summary, PEG-6 has been shown to produce minimal non-specific binding on the T-SAM, conferring most robustness towards analysis in biologically relevant matrices, and an optimum spacer length of the probes studied for the proposed sensing strategy, resulting in a clinically relevant LoD of 200 pM for the protease enzyme trypsin.

## **Acknowledgements**

The authors acknowledge financial support from the EPSRC-funded Implantable Microsystems for Personalised Anti-Cancer Therapy (IMPACT) programme [Grant ref. EP/K034510/1].

## **Appendix A. Supplementary material**

## **References**

[1] C. López-Otín, L.M. Matrisian, Emerging roles of proteases in tumour suppression, *Nat. Rev. Cancer* 7 (2007) 800-808.

- [2] S.D. Mason, J.A. Joyce, Proteolytic networks in cancer, *Trends Cell Biol.* 21 (2011) 228-237.
- [3] J. Li, J. Yuan, Caspases in apoptosis and beyond, *Oncogene* 27 (2008) 6194-6206.
- [4] J. Li, S. Li, C.F. Yang, Electrochemical Biosensors for Cancer Biomarker Detection, *Electroanalysis* 24 (2012) 2213-2229.
- [5] S.N. Topkaya, M. Azimzadeh, M. Ozsoz, Electrochemical Biosensors for Cancer Biomarkers Detection: Recent Advances and Challenges, *Electroanalysis* 28 (2016) 1402-1419.
- [6] A. Vasilescu, W. Schuhmann, S. Gaspar, Recent Progress in the Electrochemical Detection of Disease-Related Diagnostic Biomarkers in: S. Peteu, P. Vadgama (Eds.), *Detection Challenges in Clinical Diagnostics*, RSC, Cambridge, 2013, pp. 89-128.
- [7] M. Labib, P.O. Shipman, S. Martić, H.B. Kraatz, Towards an early diagnosis of HIV infection: an electrochemical approach for detection of HIV-1 reverse transcriptase enzyme, *Analyst* 136 (2011) 708-715.
- [8] Q. Liu, J. Wang, B.J. Boyd, Peptide-based biosensors, *Talanta* 136C (2015) 114-127.
- [9] J. Adjémian, A. Anne, G. Cauet, C. Demaille, Cleavage-Sensing Redox Peptide Monolayers for the Rapid Measurement of the Proteolytic Activity of Trypsin and  $\alpha$ -Thrombin Enzymes, *Langmuir* 26 (2010) 10347-10356.
- [10] A. Anne, A. Chovin, C. Demaille, Optimizing electrode-attached redox-peptide systems for kinetic characterization of protease action on immobilized substrates. Observation of dissimilar behavior of trypsin and thrombin enzymes, *Langmuir* 28 (2012) 8804-8813.
- [11] E. González-Fernández, N. Avlonitis, A.F. Murray, A.R. Mount, M. Bradley, Methylene blue not ferrocene: Optimal reporters for electrochemical detection of protease activity, *Biosens. Bioelectron.* 84 (2016) 82-88.
- [12] G. Liu, J. Wang, D.S. Wunschel, Y. Lin, Electrochemical proteolytic beacon for detection of matrix metalloproteinase activities, *J. Am. Chem. Soc.* 128 (2006) 12382-12383.

- [13] D.S. Shin, Y. Liu, Y. Gao, T. Kwa, Z. Matharu, A. Revzin, Micropatterned surfaces functionalized with electroactive peptides for detecting protease release from cells, *Anal. Chem.* 85 (2013) 220-227.
- [14] H. Xiao, L. Liu, F. Meng, J. Huang, G. Li, Electrochemical approach to detect apoptosis, *Anal. Chem.* 80 (2008) 5272-5275.
- [15] Y. Xue, M.L. O'Mara, P.P.T. Surawski, M. Trau, A.E. Mark, Effect of Poly(ethylene glycol) (PEG) Spacers on the Conformational Properties of Small Peptides: A Molecular Dynamics Study, *Langmuir* 27 (2011) 296-303.
- [16] X. Han, Y. Liu, F.-G. Wu, J. Jansensky, T. Kim, Z. Wang, et al., Different Interfacial Behaviors of Peptides Chemically Immobilized on Surfaces with Different Linker Lengths and via Different Termini, *J. Phys. Chem. B* 118 (2014) 2904-2912.
- [17] A.A. Lubin, B. Vander Stoep Hunt, R.J. White, K.W. Plaxco, Effects of Probe Length, Probe Geometry, and Redox-Tag Placement on the Performance of the Electrochemical E-DNA Sensor, *Anal. Chem.* 81 (2009) 2150-2158.
- [18] Y. Wu, R.Y. Lai, Effects of DNA Probe and Target Flexibility on the Performance of a "Signal-on" Electrochemical DNA Sensor, *Anal. Chem.* 86 (2014) 8888-8895.
- [19] S. Martić, M. Labib, D. Freeman, H.-B. Kraatz, Probing the Role of the Linker in Ferrocene-ATP Conjugates: Monitoring Protein Kinase Catalyzed Phosphorylations Electrochemically, *Chem. Eur. J.* 17 (2011) 6744-6752.
- [20] S. Campuzano, F. Kuralay, M.J. Lobo-Castañón, M. Bartošík, K. Vyavahare, E. Paleček, et al., Ternary monolayers as DNA recognition interfaces for direct and sensitive electrochemical detection in untreated clinical samples, *Biosens. Bioelectron.* 26 (2011) 3577-3583.
- [21] S. Campuzano, F. Kuralay, J. Wang, Ternary monolayer interfaces for ultrasensitive and direct bioelectronics detection of nucleic acids in complex matrices, *Electroanalysis* 24 (2012) 483-493.

- [22] V. Dharuman, B.Y. Chang, S.M. Park, J.H. Hahn, Ternary mixed monolayers for simultaneous DNA orientation control and surface passivation for label free DNA hybridization electrochemical sensing, *Biosens. Bioelectron.* 25 (2010) 2129-2134.
- [23] P. Jolly, N. Formisano, J. Tkáč, P. Kasák, C.G. Frost, P. Estrela, Label-free impedimetric aptasensor with antifouling surface chemistry: A prostate specific antigen case study, *Sens. Actuators B* 209 (2015) 306-312.
- [24] O.Y. Henry, J.L. Sanchez, C.K. O'Sullivan, Bipodal PEGylated alkanethiol for the enhanced electrochemical detection of genetic markers involved in breast cancer, *Biosens. Bioelectron.* 26 (2010) 1500-1506.
- [25] A. McQuistán, A.J. Zaitouna, E. Echeverria, R.Y. Lai, Use of thiolated oligonucleotides as anti-fouling diluents in electrochemical peptide-based sensors, *Chem. Commun.* 50 (2014) 4690-4692.
- [26] R. Woods, Chemisorption at electrodes, hydrogen and oxygen on noble metals and their alloys in: A.J. Bard (Ed.) *Electroanalytical chemistry*, Marcel Dekker, New York, 1976, pp. 1-162.
- [27] J.M. Artigas, M.E. Garcia, M.R. Faure, A.M. Gimeno, Serum trypsin levels in acute pancreatic and non-pancreatic abdominal conditions, *Postgrad. Med. J.* 57 (1981) 219-22.
- [28] J. Labuda, A. M. Oliveira Brett, G. Evtugyn, M. Fojta, M. Mascini, M. Ozsoz, et al., *Electrochemical nucleic acid-based biosensors: Concepts, terms, and methodology (IUPAC Technical Report)*, *Pure Appl. Chem.* 82 (2010) 1161-1187.